

## Silicon Photonics for Mid-Infrared Sensing

D. J. Rowe, Y. Qi, V. Mittal, A. Osman, Z. Qu,  
Y. Wu, M. Banakar, J. Soler Penades, J. S. Wilkinson,  
M. Nedeljkovic, G. Z. Mashanovich  
Optoelectronics Research Centre  
University of Southampton  
Southampton, UK  
e-mail: g.mashanovich@soton.ac.uk

A. Sánchez-Postigo, J. G. Wangüemert-Pérez,  
A. Ortega-Moñux, R. Halir, Í. Molina-Fernández  
Dpto. Ingeniería de Comunicaciones  
Universidad de Málaga  
Malaga, Spain

**Abstract**—In this paper, we review our recent work on Si and Ge material platforms suitable for mid-infrared sensing. We investigate Silicon-on-Insulator, Germanium-on-Silicon, suspended Si and suspended Ge. Design, fabrication and characterisation results for various passive devices are discussed. We also show preliminary results on integration of microfluidic channels with the Silicon-on-Insulator platform.

**Keywords**—silicon; germanium; mid-infrared; waveguides.

### I. INTRODUCTION

The mid-infrared (MIR) wavelength region contains strong absorption bands of many molecules and substances and is therefore of great interest for various sensing applications [1]. Silicon and germanium are suitable material platforms for the MIR as they are transparent in this wavelength range and are readily available with well established fabrication techniques mostly employed for the realisation of near-IR photonic devices [2].

As the MIR wavelength range is very broad (2-15  $\mu\text{m}$ ) and different applications can target different wavelengths within the MIR, development of non-standard material platforms may be needed. SOI is the most popular platform in the NIR and is low loss up to  $\sim 3.8 \mu\text{m}$  [3]. To utilise the full transparency of Si, buried oxide layer can be removed resulting in a suspended Si structure. In this paper we report our approach based on subwavelength gratings [4][5]. Several research groups have reported Ge-on-Si and SiGe waveguides with operation up to 8.5  $\mu\text{m}$  [6-8]. However, such waveguides have limited evanescent field which may result in low sensitivity of transducers based on these platforms. Suspended Ge is an alternative platform for sensing [9] and here we discuss our preliminary result on this platform. Finally, we show integration of microfluidic PDMS channels and SOI waveguides and measurement of aqueous solutions of IPA.

The paper is organised as following. A review of several MIR platforms is given in Section II. Section III describes suspended Si and suspended Ge platforms. Integration of MIR photonic circuits with microfluidic channels is given in Section IV. Finally, Section V contains conclusions.

### II. STANDARD PLATFORMS

The SOI platform has been extensively used for NIR devices, photonic integrated circuits and systems [10]. It is therefore a preferred platform in silicon photonics and we have conducted an extensive investigation into its suitability for the MIR. We have shown that this platform can be used up to  $\sim 4 \mu\text{m}$  due to large  $\text{SiO}_2$  material loss beyond  $\sim 3.6 \mu\text{m}$  [3]. A number of MIR devices have been realised in this platform, for example waveguides with loss of  $\sim 1 \text{ dB/cm}$ , spectrometers [2], modulators [9], detectors [11][12], integrated sources [13] etc. This platform can also be used for sensing as shown for example in [14] and in Section IV of this paper. To increase refractive index contrast and also transparency range, pedestal Si and suspended Si can be used as shown in Section II.

The main appeal of Ge as a MIR material is its superior spectral transparency compared to Si that spans from 2 to 15  $\mu\text{m}$ . Ge also has other interesting characteristics such as larger carrier mobility, thermo-optic and non-linear coefficients compared to Si. The most popular approach for fabrication of Ge-based MIR platform has been CVD growth of Ge on Si wafers. Various Ge thicknesses have been used with reported losses typically around 2 dB/cm and with best results as low as 0.6 dB/cm [15].

Ge-rich SiGe waveguides have also been demonstrated and sub dB/cm losses shown [8]. The main advantage of this approach is the possibility to have a gradual change of Ge concentration in the SiGe alloy thus reducing defect concentration that can affect the GOS platform losses.

Although these platforms should have low losses up to 11 or 12  $\mu\text{m}$ , larger values have been observed beyond 8.5-9  $\mu\text{m}$  [6-8] and therefore further investigation is needed. These platforms have another drawback: to enable low propagation losses thicker Ge and SiGe top layers are required resulting in high optical mode confinement in the core and low evanescent field as shown in Figure 1 for a GOS waveguide. This results in low interaction of the optical mode with an analyte and thus lower sensitivity. Suspended Ge can offer solution to this problem as discussed in the next section.

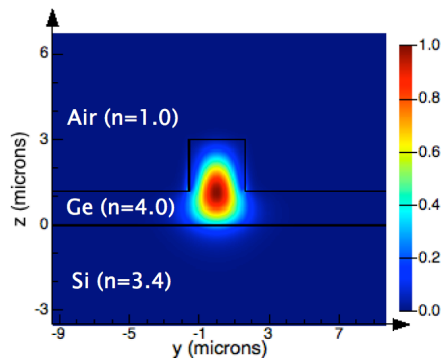


Figure 1. GOS waveguide: optical mode is well confined in the waveguide resulting in low evanescent field.

### III. SUSPENDED PLATFORMS

#### A. Suspended Si

Si is transparent up to 8  $\mu\text{m}$  and to realise Si-based photonics circuits that operate to a wavelength as long as 8  $\mu\text{m}$  there are two solutions: a) Si is bonded to a substrate that has the same or larger transparency range and b) the buried oxide (BOX) in SOI is removed and suspended Si formed. Here, we discuss b).

The most obvious solution is to form a rib waveguide and holes on both sides of the rib that can be used for wet selective etching of the BOX layer. This requires two dry etch steps to form the rib and holes and also careful positioning of the holes such not to cause scattering of the optical mode. It can also result in bending of the slab region for larger structures, such as Multi-Mode Interference (MMI) splitters or Mach-Zehnder Interferometers (MZIs), depending on the thickness of the slab region.

A better solution is to place the holes in close proximity to the core, to increase the mode-analyte interaction, to improve mechanical stability and to simplify the fabrication process. We have developed such an approach based on subwavelength gratings as shown in Figure 2. The subwavelength gratings act as lateral claddings and access points for HF removal of the BOX.

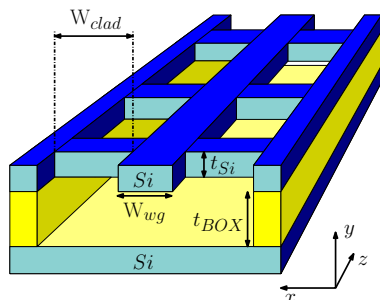


Figure 2. Suspended Si waveguide with subwavelength grating cladding.

There are several contradictory requirements when designing such structures. To reduce scattering caused by the sidewall roughness the waveguide core  $W_{wg}$  should be wide. This can result in multimode propagation and/or downward

bending of the waveguide. The cladding width  $W_{clad}$  should be relatively large to reduce the leakage loss but on the other hand small to reduce downward bending. Subwavelength holes should be large enough to enable liquid HF penetration and subsequent BOX removal, however also small enough not to reduce Si side supports that are important to mechanical stability of the structure. If these Si supports are too wide they can increase mode leakage to the slab region.

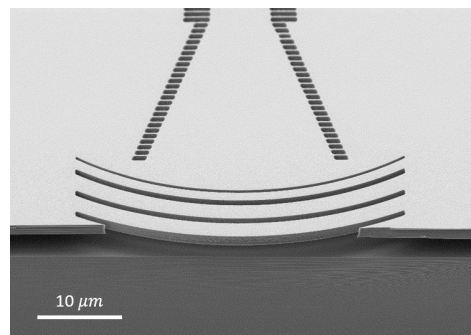


Figure 3. Part of a suspended grating coupler for suspended Si photonic circuits operating at a wavelength of 7.7  $\mu\text{m}$  [16].

It is clear from the previous paragraph that extensive simulations are required to optimise dimensions of various photonic devices based on the subwavelength grating design. We have conducted such an optimisation and fabricated devices operating at 3.8 [5] and 7.7  $\mu\text{m}$  [16], achieving propagation losses of 0.8 dB/cm and 3.1 dB/cm, respectively, low bending losses, low insertion losses for MMIs, MZIs, and good coupling efficiency for surface grating couplers (Figure 3). It should be pointed out that Si material loss at 7.7  $\mu\text{m}$  is 2.1 dB/cm, and leakage loss for this particular waveguide is 0.1 dB/cm, meaning that the ‘actual’ waveguide loss is 0.9 dB/cm which is very similar to the 3.8  $\mu\text{m}$  result of 0.8 dB/cm [5]. This demonstrates a robust fabrication method.

#### B. Suspended Ge

To suspend Ge, the same two approaches can be implemented: rib waveguide configuration (Figure 4) or subwavelength grating approach discussed in the previous section (Figure 2). We have applied the former, and we are currently working on the latter.

In terms of the substrate, Si or SOI can be used. In our approach, we have used the SOI substrate because it results in a well defined air channel under the Ge rib waveguide (Figure 4).

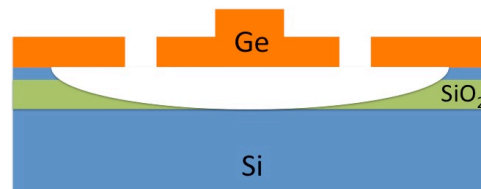


Figure 4. Suspended Ge waveguide on thin SOI platform.

The waveguides were fabricated using 6" Ge-on-SOI wafers with a 1  $\mu\text{m}$  Ge layer grown by RPCVD on 50 nm SOI. The BOX thickness was 3  $\mu\text{m}$ . Rib waveguides were designed for single mode propagation at  $\lambda = 7.7 \mu\text{m}$ . The dimensions were: height (H) = 1  $\mu\text{m}$ , width (W) = 3.5  $\mu\text{m}$  and etch depth (D) = 300 nm. The initial SOI substrate consisted of a 250 nm thick layer of Si on a 3  $\mu\text{m}$  thick layer of SiO<sub>2</sub>. It was thinned to 50nm Si using oxidation. The waveguides were patterned using e-beam lithography. They were then defined by dry etching using ICP. A second e-beam lithography step followed in order to define the holes, which were etched down to the BOX. The sample then underwent two wet etch steps. First, the sample was immersed in 1:7 HF, which removed the BOX. Then it was immersed in a 25% aqueous solution of Tetramethylammonium Hydroxide (TMAH) at room temperature, which resulted in a removal of the 50 nm thick Si layer.

The waveguides were measured using the effective cut-back method. Waveguides of different lengths were fabricated for the propagation loss measurement. The measured value was 2.65 dB/cm at  $\lambda = 7.7 \mu\text{m}$ . Our future work will address waveguides for longer wavelengths and development of other passive devices in this platform and its implementation for sensing.

#### IV. INTEGRATION WITH MICROFLUIDIC CHANNELS

Strip waveguides were fully etched in 500 nm silicon on 3  $\mu\text{m}$  silica with a silica cladding. The mode profile was optimised using Lumerical for maximum sample interaction and to prevent cross-talk. Spirals were used to reduce footprint while providing a range of interaction lengths, where the sample-waveguide interaction length was determined by a window in the silica cladding. Gratings were optimised for operation at  $\lambda = 3.8 \mu\text{m}$ .

PDMS microfluidic channels were prepared using Sylgard 184 and a 3D printed resin mould. The channel had 3000 x 100  $\mu\text{m}$  cross-section and 30 mm length. The channel was made excessively wide for simple manual alignment with the sensing windows, although we subsequently designed a mount to aid alignment and reduce channel width. An O<sub>2</sub> plasma was used for surface modification to covalently bond the PDMS and SiO<sub>2</sub> cladding.

DI water and IPA solutions were prepared at volume fractions of 20, 40, 60, 80 and 100% and delivered using a syringe pump. A tunable QCL source and detector were coupled to waveguide gratings using fluoride mid-infrared fibres. A lock-in amplifier and chopper were used to reduce noise. A LabVIEW program was used to synchronise the laser wavelength sweep with data collection.

The normalised power spectra of water-IPA solutions relative to water are shown in Figure 5, showing the expected IPA absorption at  $\lambda = 3.76 \mu\text{m}$ . All measurements were performed using a 100  $\mu\text{m}$  interaction length. By using longer interaction lengths smaller concentrations of aqueous solutions of IPA (~1%) can be achieved.

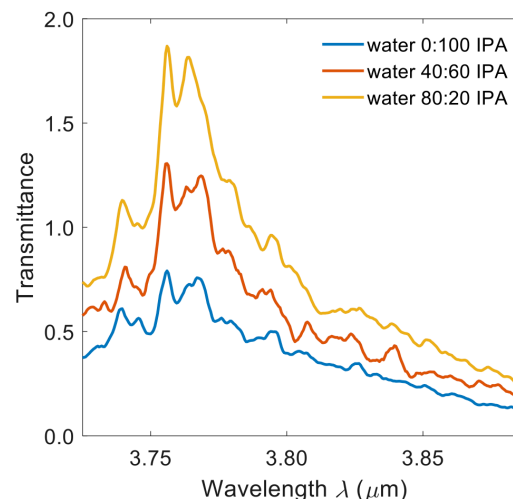


Figure 5. Transmittance of water-IPA solutions relative to water, showing the expected IPA absorption at  $\lambda = 3.76 \mu\text{m}$ .

#### V. CONCLUSIONS

Low loss waveguides and other photonic devices have been realised in SOI, GOS, suspended Si and suspended Ge platforms. Which platform will be used depends on the application in question and appropriate wavelength range. Work is underway to integrate these platforms with microfluidic channels for detection of various substances that have strong absorption bands in the MIR.

#### ACKNOWLEDGMENT

This work was supported by the EPSRC in the UK through the following projects: National Hub in High Value Photonic Manufacturing (EP/N00762X/1), Electronic-Photonic Convergence (EP/N013247/1), MIGRATION (EP/L01162X/1), and CORNERSTONE (EP/L021129/1), and by the Royal Academy of Engineering (RF201617/16/33).

#### REFERENCES

- [1] R. Soref, "Mid-infrared photonics in silicon and germanium," *Nature Photonics*, vol. 4, pp. 495-497, 2010.
- [2] G. Z. Mashanovich et al., "Silicon photonic waveguides and devices for near- and mid-IR applications," *IEEE Journal of Selected Topics in Quantum Electronics*, vol. 21, pp. 1-12, 2015.
- [3] M. Nedeljkovic et al., "Silicon photonic devices and platforms for the mid-infrared" *Optical Materials Express*, vol. 3, pp. 1205-1214, 2013.
- [4] J. Soler Penades et al., "Suspended SOI waveguide with sub-wavelength grating cladding for mid-infrared," *Optics Letters*, vol. 39, pp. 5661-5664, 2014.
- [5] J. Soler Penades et al., "Suspended silicon mid-infrared waveguide devices with subwavelength grating metamaterial cladding," *Optics Express*, vol. 24, pp. 22908-22916, 2016.
- [6] M. Brun et al., "Low loss SiGe graded index waveguides for mid-IR applications," *Optics Express*, vol. 22, pp. 508, 2014.
- [7] M. Nedeljkovic et al., "Germanium-on-silicon waveguides operating at mid-infrared wavelengths up to 8.5  $\mu\text{m}$ ," *Optics Express*, vol. 25, pp. 27431-27441, 2017.

- [8] J. M. Ramirez et al., "Graded SiGe waveguides with broadband low-loss propagation in the mid infrared," *Optics Express*, vol. 26, pp. 870-877, 2018.
- [9] G. Z. Mashanovich et al., "Group IV mid-infrared photonics," *Optical Materials Express* (in press)
- [10] D. Thomson et al., "Roadmap on silicon photonics," *Journal of Optics*, vol. 18, 073003, 2016.
- [11] J. J. Ackert, et al., "High-speed detection above the telecommunication windows with monolithic silicon photodiodes," *Nature Photonics*, vol. 9, pp. 393-396, 2015.
- [12] M. Muneeb et al., "III-V-on-silicon integrated micro-spectrometer for the 3  $\mu\text{m}$  wavelength range," *Optics Express*, vol. 24, pp. 9465-9472, 2016.
- [13] A. Spott et al., "Quantum cascade laser on silicon," *Optica*, vol. 3, p. 545, 2016.
- [14] P. Tai Lin et al., "Label-free glucose sensing using chip-scale mid-infrared integrated photonics," *Advanced Materials*, vol. 4, pp. 1755-175, 2016.
- [15] M. Nedeljkovic et al., "Surface-grating-coupled low-loss Ge-on-Si rib waveguides and multimode interferometers," *IEEE Photonics Technology Letters*, vol. 27, pp. 1040-1043, 2015.
- [16] J. Soler Penadés et al., "Suspended silicon waveguides for long-wave infrared wavelengths," *Optics Letters*, vol. 43, pp. 795-798, 2018.